

Contract No:

This document was prepared in conjunction with work accomplished under Contract No. 89303321CEM000080 with the U.S. Department of Energy (DOE) Office of Environmental Management (EM).

Disclaimer:

This work was prepared under an agreement with and funded by the U.S. Government. Neither the U.S. Government or its employees, nor any of its contractors, subcontractors or their employees, makes any express or implied:

- 1) warranty or assumes any legal liability for the accuracy, completeness, or for the use or results of such use of any information, product, or process disclosed; or
- 2) representation that such use or results of such use would not infringe privately owned rights; or
- 3) endorsement or recommendation of any specifically identified commercial product, process, or service.

Any views and opinions of authors expressed in this work do not necessarily state or reflect those of the United States Government, or its contractors, or subcontractors.

CORROSION ASSESSMENT MODELS FOR PREDICTING REMAINING STRENGTH OF CORRODED THICK-WALLED PIPELINES

Xian-Kui Zhu, Bruce Wiersma, William R. Johnson, Robert Sindelar

Materials Technology
Savannah River National Laboratory
Aiken, SC 29808, USA

ABSTRACT

Corrosion is a major threat to pipeline integrity. Over the past half century, many corrosion assessment models have been developed for determining the remaining strength of corroded pipelines, including the traditional industry codes of ASME B31.G, Modified B31.G and PRCI RSTRENG, and numerous newer corrosion criteria, such as LPC, PCORRC and their modified models. However, all available corrosion assessment models are applicable to large diameter, thin-walled line pipes with a diameter to wall thickness ratio $D/t \geq 20$. In practice, there are a lot of small-diameter, thick-walled pipelines with a D/t ratio < 20 , and thus an adequate corrosion assessment model is needed for predicting remaining strength for corroded thick-walled pipelines.

This paper first reviews the burst pressure models for defect-free thin and thick-walled pipelines and a variety of corrosion assessment models for thin-walled pipelines. On this basis, three corrosion assessment models are developed for thick-walled pipelines in terms of the average shear stress yielding theory. A large set of burst test data is employed to evaluate and validate the proposed corrosion assessment models for thick-walled pipelines in a wide range of pipeline steel grades. The comparison shows that the proposed thick-wall corrosion models more accurately predict the remaining strength for both thin and thick-walled pipelines with corrosion defects.

KEYWORDS: Pipeline, corrosion defect, remaining strength, corrosion assessment model, thick-wall theory

1. INTRODUCTION

Pipeline systems are an important infrastructure in the energy sector that provides economic and safe transportation of large volumes of crude oil or natural gas over long distances to meet increasing energy demands. The pipelines are made of carbon steels, and most pipelines are buried underground per regulations. Due to underground water or sour soils, buried steel pipes are susceptible to external corrosion attack that threatens

pipeline integrity. It has been recognized that corrosion is one of leading causes of failure for aging pipelines, and thus corrosion assessment is critical for pipeline operators to manage their asset integrity for buried pipelines [1].

For determining burst strength of pressure vessels, numerous empirical, analytical or numerical methods [4] have been developed for defect-free cylinders subject to internal pressure, as reviewed by Christopher et al. [5] for thick-walled pressure vessels and Zhu and Leis [3] for thin-walled line pipes. In order to consider the material plastic flow effect, Zhu and Leis [4, 5] developed an average shear stress yielding theory and obtained a Zhu-Leis solution of burst pressure for thin-walled pipelines. Experimental comparisons [3, 5] showed that the Zhu-Leis solution is the most accurate prediction of burst pressure for defect-free thin-walled pipes. Moreover, Zhu [6] evaluated strength criteria and plastic flow criteria used in pressure vessel design and analysis.

The pipeline industry began to investigate the threat posed by corrosion in the late 1960s, and the early experimental data and analytical results were published in the 1970s [7 - 9]. Full-scale burst tests were conducted on pipe segments removed from service, and burst pressure data were trended as a function of the length and depth of corrosion defects for vintage natural gas (NG) pipeline steels. The trending function originated in the NG-18 equations [8 - 9] were developed at Battelle in the early 1970s for determining fracture failure of pipelines containing cracks. Based on the NG-18 equation for collapse-controlled failure, the American Society for Mechanical engineers (ASME) in cooperation with the oil & gas industry codified an empirical corrosion assessment method in 1984, which was published as B31G [10]. To reduce the conservatism, Modified B31G was published in 1989 and revised in 2009.

With advances of steel making technology, both strength and toughness of modern pipeline steels have significantly improved, and many high-strength pipeline grades, such as X70 and X80, are being utilized today. Accordingly, over the past decades, many improved corrosion assessment models [11] were developed for better managing high-strength pipelines. Among

them, the ultimate tensile stress (UTS)-based models can determine a more accurate remaining strength of corroded pipelines, and thus has been accepted by British Standard BS 7910 [12] and American Standard API 579 [13] for a fitness for service (FFS) assessment of pressure vessels. However, ASME B31G and Modified B31G remain in use today in the pipeline industry, even though these models are conservative.

Recently, Zhu [14, 15] delivered a review on the primary existing corrosion assessment models for metal-loss or corrosion defects in pipelines and discussed some practical challenges facing the oil and gas industry. Zhu and Wiersma [16] presented a recent progress of corrosion assessment model development for determining the remaining strength of corroded pipelines, including newer plastic flow models and machine learning models developed at US DOE Savannah River National Laboratory (SRNL). Zhu [17] discussed numerical approaches used to predict burst pressure for pipelines with corrosion defects. Leis et al. [18] reported numerical results that minimized the uncertainty of ASME B31G model. Zhou and Huang [19] assessed the errors in the corrosion models. Amaya-Gomez et al. [20] analyzed the reliability of the corrosion models, while Bhardwaj et al. [21] quantified the uncertainty of burst pressure models for corroded pipelines. However, all available corrosion models are applicable only to thin-walled pipelines or cylindrical pressure vessels. To date, a corrosion assessment model for thick-walled pipelines is unavailable.

To meet this need, the present paper reviews burst pressure models for defect-free thin-walled and thick-walled pipelines as well as a variety of corrosion assessment models for thin-walled pipelines. On this basis, three corrosion assessment models are proposed for predicting remaining strength of corroded thick-walled pipelines in terms of the average shear stress yielding theory. A large burst test database is then employed to evaluate and validate the proposed corrosion assessment models for corroded thick-walled pipelines with a wide range of pipeline steel grades. The comparison shows that the proposed corrosion models for thick-walled pipes more accurately predict the remaining strength for corroded thin-walled and thick-walled pipelines.

2. BURST MODELS FOR DEFECT-FREE PIPES

The burst pressure prediction for defect-free pipes is the basis to develop corrosion models for assessing corroded pipeline integrity [15]. The reference stress of a corrosion model is defined by the burst strength of defect-free pipes. This section briefly reviews the existing strength and flow models for burst pressure of defect-free thin-walled pipes and the newer flow models for defect-free thick-walled pipes.

2.1. Strength models for thin-walled pipes

For defect-free, large diameter thin-walled pipes, four strength models [6] of burst pressure were obtained in terms of the UTS as well as Tresca, von Mises, Zhu-Leis, and flow stress criteria [9]. The Tresca strength (P_0), Mises strength (P_{M0}), Zhu-Leis strength (P_{A0}) and flow strength (P_{f0}) are determined as:

- 1). Tresca strength solution:

$$P_0 = \frac{2t}{D} \sigma_{uts} \quad (1)$$

- 2). von Mises strength solution:

$$P_{M0} = \frac{4t}{\sqrt{3}D} \sigma_{uts} \quad (2)$$

- 3). Zhu-Leis strength solution:

$$P_{A0} = \frac{1}{2} \left(1 + \frac{2}{\sqrt{3}} \right) \frac{2t}{D-t} \sigma_{uts} \quad (3)$$

- 4). Flow stress-based failure solution:

$$P_{f0} = \frac{2t}{D} \sigma_{flow} \quad (4)$$

where D ($D-t$) is the outside (mean) diameter, and t is the wall thickness of the pipe. The flow stress $\sigma_{flow} = (\sigma_{ys} + \sigma_{uts})/2$, σ_{ys} is the yield stress (YS) and σ_{uts} is the UTS. Zhu-Leis strength solution in Eq. (3) was determined from the average shear stress strength theory [5, 6]. Equations (1) to (3) show that the Zhu-Leis strength solution is the averaged result of Tresca and von Mises strength solutions. Tresca solution in Eq. (1) is often referred to as *Barlow strength* in the pipeline industry.

To evaluate the accuracy of four strength models in Eqs (1) to (4), experimental data for burst pressure (P_b) for more than 100 full-scale tests of thin-walled cylindrical pressure vessels made of carbon steel were compared with those predicted from the four strength criteria, as shown in Fig. 1. All materials used in the experiments are ductile steels, with strain hardening exponents, n , that range from 0.02 to 0.18, that represents low to high-strength pipeline steels from Grade B to X120.

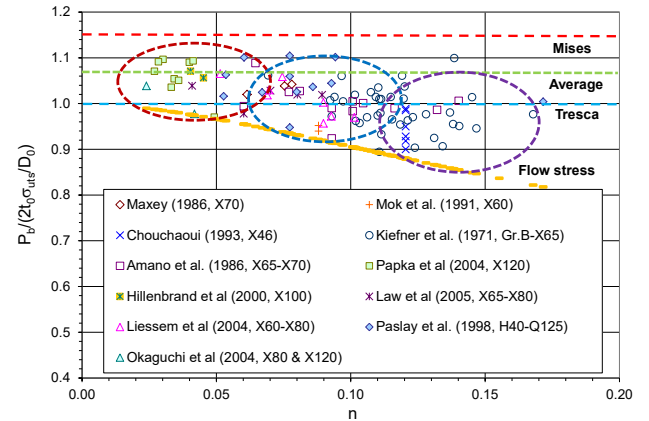


Figure 1. Comparison of experimental burst pressure data and predictions by von Mises, Zhu-Leis, Tresca, and flow stress criteria for various pipeline steels [6]

Experimental details and References cited in Fig. 1 were described by Zhu and Leis [6]. The points in the figure are experimental data, and the lines are burst pressure predictions. Three circles indicate three groups of test data. The purple, blue and red circles represent test data for low, intermediate, and high strength carbon steels, respectively. Four dashed lines in red, green, blue, and yellow denote the burst pressure predictions, by the von Mises, Zhu-Leis, Tresca, and flow stress criteria, respectively. This figure shows that (1) von Mises strength criterion overestimates burst pressure for all steels, (2) Zhu-Leis

strength criterion is good for high-strength steels but overestimates burst pressure for low-strength steels, (3) Tresca strength criterion adequately predicts burst pressure for intermediate-strength steels, and (4) the flow stress criterion predicts the most conservative results for all steels.

Also evident in Fig. 1, the burst pressure decreases with increasing strain hardening exponent. Except for the flow stress criterion, however, the other three strength solutions did not consider the effect of strain hardening on burst pressure. To improve these strength solutions, the flow theory of plasticity [4] is needed to use for developing more accurate burst pressure solutions.

2.2. Flow models for thin-walled pipes

The Tresca theory and von Mises theory are two classical theories of plasticity developed for describing nonlinear plastic deformation in a ductile material during loading. They can determine two extreme solutions of burst pressure for the same pipe. To predict a more accurate burst failure, Zhu and Leis [3, 4] developed an intermediate multi-axial flow theory of plasticity, that is, the average shear stress flow theory or Zhu-Leis flow theory. For a power-law hardening material, these three flow theories of plasticity determines three flow solutions of burst pressure that are called Tresca, Zhu-Leis and von Mises flow solutions:

$$P_T = \left(\frac{1}{2}\right)^{n+1} \frac{4t}{D-t} \sigma_{uts} \quad (5)$$

$$P_A = \left(\frac{2+\sqrt{3}}{4\sqrt{3}}\right)^{n+1} \frac{4t}{D-t} \sigma_{uts} \quad (6)$$

$$P_M = \left(\frac{1}{\sqrt{3}}\right)^{n+1} \frac{4t}{D-t} \sigma_{uts} \quad (7)$$

where n is the strain hardening exponent that can be measured from a tensile test or estimated from a yield to tensile strength (Y/T) ratio of the material [22].

The experimental data of burst pressure shown in Fig. 1 were reused here to validate the three flow theories, as shown in Figure 2. This figure shows that (1) all test data and burst pressure predictions are functions of the strain hardening exponent n and decrease with an increase in n , (2) von Mises flow solution is an upper bound prediction, (3) Tresca flow solution is a lower bound prediction, and (4) Zhu-Leis flow solution is an intermediate prediction that matches well with the burst data on average. Thus, those experiments validated the Zhu-Leis flow theory and its associated burst pressure solution for defect-free thin-walled pipes.

Using other full-scale test databases, Seghier et al. [23], Zimmermann et al [24], Zhou and Huang [25] and Bony et al. [26] all confirmed that the average shear stress yielding criterion is the best criterion, and that the Zhu-Leis flow solution is the most accurate burst pressure prediction for thin-walled pipes. As a result, Zhu-Leis flow theory [6] filled the technical gap between the classical Tresca and von Mises theories and determined a more accurate burst pressure solution.

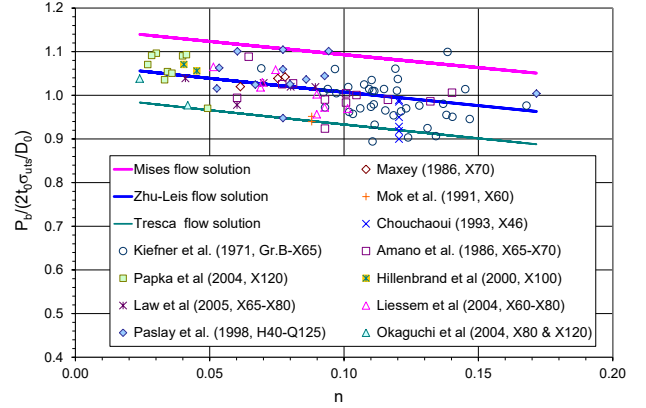


Figure 2. Comparison of the flow solutions and experimental data for various carbon steels [3]

2.3. Flow models for thick-walled pipes

The flow models of burst pressure discussed above were based on the thin-walled shell theory, where axial and hoop stresses were assumed to be constant through the wall thickness of the pipe, and thus are applicable to thin-walled pipes with $D/t \geq 20$. In practice, there are many heavy-walled line pipes with a wall thickness to be large than 20 mm or 40 mm [27], leading to $D/t < 20$. In this case, the thin-walled shell theory becomes invalid, and the thick-walled shell theory should be applied, where the axial and hoop stresses are not constant through the wall thickness, and the wall thickness becomes an important factor for pipe design or integrity assessment.

In order to obtain a burst pressure solution for defect-free thick-walled pipes, Zhu et al. [28] recently proposed a two-parameter based flow stress, and then developed a new strength theory that can predict plastic collapse of a metallic pressure vessel. On this basis, they obtained the following burst pressure solution for defect-free thick-walled cylinders or pipes:

$$P_b = 2 \left(\frac{K}{2}\right)^{n+1} \sigma_{uts} \ln \left(\frac{D_o}{D_i}\right) \quad (8)$$

where K is a constant that is related to the yield criterion:

$$K = \begin{cases} 1, & \text{for Tresca yield criterion} \\ \frac{2}{\sqrt{3}}, & \text{for von Mises yield criterion} \\ \frac{1}{2} + \frac{1}{\sqrt{3}}, & \text{for Zhu-Leis yield criterion} \end{cases} \quad (9)$$

and D_o/D_i is the outside to inside diameter ratio of the pipe.

Comparing the thick-wall burst solution in Eq. (8) with the corresponding thin-wall burst solution in Eqs (5) – (7) shows that the reference stresses are the same for the thin-walled and thick-walled shell theories, but the geometry terms are different. For the thin-walled shell theory, the geometry term is $2t/D_m$ if the mean diameter $D_m = D-t$ is used, or $2t/D$ if the outside diameter is used. For the thick-walled shell theory, the geometry term is $\ln(D_o/D_i)$. Figure 3 compares the variation of these three geometry terms with the diameter ratio. As evident in this figure, the geometry term $2t/D_m$ is very close to $\ln(D_o/D_i)$ for the

diameter ratio up to 1.4 (or $D/t = 7$), where the error is insignificant and less 1.0%, and the error is even smaller and less than 0.1% if $D/t \geq 20$. Thus, this observation suggests that the mean diameter D_m should be used in the thin-walled shell theory, and the thin-wall burst pressure solutions can be very accurate if $D/t \geq 20$, and remain practically accurate if $7 < D/t < 20$. In contrast to this, if the outside diameter is used, the difference between the two geometry terms $2t/D$ and $\ln(D_o/D_i)$ can be very large and increases as the diameter ratio increases. The error is less 1% only for very thin-walled pipes with $D_o/t > 100$, and reaches 5.1% at $D_o/t = 20$. As such, the outside diameter is not recommended for use in pipeline design or assessment, but may be used to approximate the result for engineering purposes.

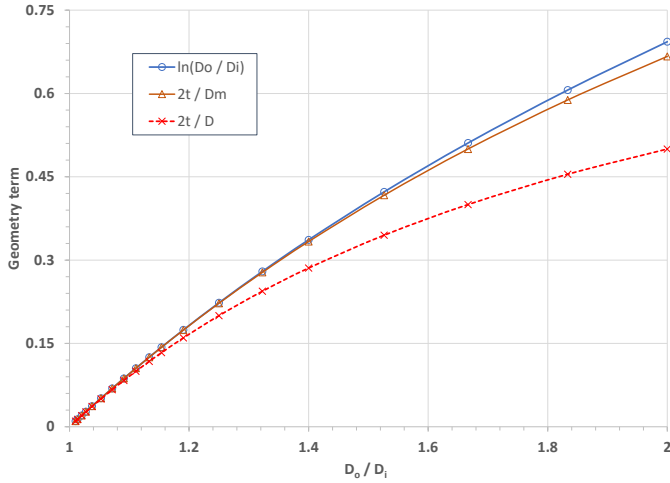


Figure 3. Comparison of three geometry terms used in the burst pressure solutions for thin and thick-walled pipes

Figure 4 compares the Zhu-Leis burst pressure solutions predicted from Eq. (6) and Eq. (8) with the full-scale burst data (as shown in Fig. 1 with limited burst data for thick-walled pipes) as a function of D/t . From this figure, it is observed that:

- (1) The newly proposed Zhu-Leis solution of burst pressure for thick-walled pipes in Eq. (8) is very accurate and closely matches the burst pressure data for all pipes with a wide range of D/t ratios, including thin to thick walls.
- (2) For thin-walled pipes with $D/t > 30$, all burst pressures are near to or less than 5,000 psi (34.47 MPa). The Zhu-Leis burst pressure solution from the thin-walled shell theory is very close to that for the thick-walled theory.
- (3) For pipes with intermediate-wall thickness of $7 < D/t < 30$, all burst pressures are larger than 5,000 psi (34.47 MPa). The D_m -based Zhu-Leis solution for thin-walled pipes is comparable to Zhu-Leis burst pressure solution for thick-walled pipes.
- (4) In contrast, the D_o -based Zhu-Leis solutions for thin-wall pipes are significantly lower than those for the thick-wall pipes with $D/t < 20$. As a result, the D_m -based rather than D_o -based Zhu-Leis solution should be used generally.

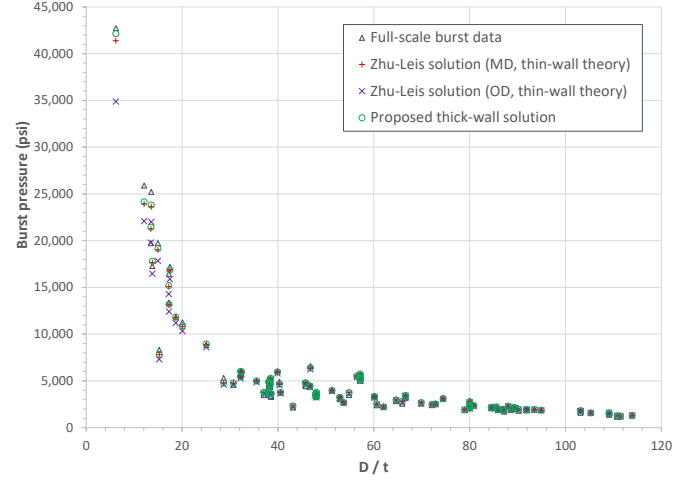


Figure 4. Comparison of predicted and measured burst pressures as a function of D/t ratio [28]

3. CORROSION MODELS FOR THIN-WALLED PIPES

Corrosion defects in aging pipelines may have complex size, shape, location and orientation. Only axially oriented, isolated corrosion defects in pipelines subject to internal pressure are considered in this work. Other anomalies and loading conditions will not be considered.

A general expression of burst pressure for a corrosion defect in thin-walled pipelines can be expressed as [13, 15]:

$$P_b = S_R \times 2t/D \times f(\text{defect geometry}) \quad (10)$$

where S_R is a reference stress, $2t/D$ denotes the geometry term for a thin-walled pipe, and f is a function of the defect geometry (depth d , length L and width W). In many cases, defect width has a minor effect, and f can be simplified as $f(d/t, L/\sqrt{Dt})$. Absent a defect, Eq. (10) reduces to the burst pressure solution for a defect-free pipe, and thus the S_R is equal to burst strength of the defect-free pipe.

Based on different definitions of the reference stress, existing corrosion assessment models can be categorized into three generations [15]. Examples of each are presented next.

3.1. The first-generation models (1960s – 1980s)

The first-generation models were developed empirically from full-scale tests in the 1960s to 1980s with $S_R = \text{flow stress}$.

3.1.1. ASME B31G

Based on full-scale burst test data obtained in the early 1970s for pipeline steels up to X65, Maxey et al. [8-9] developed semi-empirical equations (i.e., NG-18 equations) to predict burst pressure of pipelines with cracks. On this basis, a corrosion assessment method was codified by ASME in 1984 and published as B31G [10]. For actual short corrosion defects, the corroded area was assumed to be parabolic in shape with a curved bottom, and burst pressure of the corroded thin-walled pipeline was determined as:

$$p_b = \frac{2t\sigma_f}{D} \left[\frac{1-(2/3)(d/t)}{1-(2/3)(d/t)/M} \right], \quad \text{for } L \leq \sqrt{20Dt} \quad (11)$$

where the defect depth is limited to 80% of t , or $d/t \leq 0.8$.

For long corrosion defects, corrosion shape was simplified to be a rectangle with a flat bottom, and so Eq. (11) becomes:

$$p_b = \frac{2t\sigma_f}{D} \left[1 - \frac{d}{t} \right], \quad \text{for } L > \sqrt{20Dt} \quad (12)$$

In the equations above, the flow stress $\sigma_f = 1.1 \text{ SMYS}$, where SMYS is the specified minimum yield stress, and M is a Folia's bulging factor [29] and expressed as:

$$M = \sqrt{1 + 0.8 \left(\frac{L}{\sqrt{Dt}} \right)^2} \quad (13)$$

Note that the ASME B31G model was calibrated with vintage pipeline grades up to X65, and thus may be inadequate to use for modern pipeline steels like X80 or X100.

3.1.2. Modified B31G (0.85 dL)

Applications showed that ASME B31G model can be overly conservative [30], and thus a modified B31G was proposed by PRCI through a series of full-scale burst tests [31]. Then, the burst pressure was modified as:

$$p_b = \frac{2t\sigma_f}{D} \left[\frac{1-0.85(d/t)}{1-0.85(d/t)/M} \right] \quad (14)$$

where the defect depth is limited to 80% of t or $d/t \leq 0.8$, the flow stress was redefined as $\sigma_f = \text{SMYS} + 69 \text{ (MPa)}$, and the bulging factor M was modified as:

$$M = \sqrt{1 + 0.6275 \left(\frac{L}{\sqrt{Dt}} \right)^2 - 0.003375 \left(\frac{L}{\sqrt{Dt}} \right)^4}, \quad \text{if } L \leq \sqrt{50Dt} \quad (15a)$$

$$M = 3.3 + 0.032 \left(\frac{L}{\sqrt{Dt}} \right)^2, \quad \text{if } L > \sqrt{50Dt} \quad (15b)$$

Note that the 0.85 factor used in Modified B31G reduces the model conservatism. The Modified B31G model was accepted in the newer edition of ASME B31G-2009 [10] and in Level-1 procedure of API 579-2016 [13].

3.1.3. PRCI RSTRENG (effective area model)

A more realistic corrosion defect has a river bottom profile. Kiefner and Vieth [32] proposed an effective area method to improve the estimate the remaining strength:

$$P_b = \frac{2t\sigma_f}{D} \left[\frac{1-A_d/A_0}{1-A_d/A_0M} \right] \quad (16)$$

where the flow stress and the bulging factor are the same as defined for Modified B31G, A_d denotes the effective area of a complex corrosion defect profile, and $A_0 = tL$ is the axial cross-section area of the defect. This model calculates a more accurate corroded area using the discrete approach, and thus a more accurate burst pressure for a real corrosion defect. A computer code RSTRENG [32] was also developed to predict more accurate burst pressure results for corroded pipes. This effective area model was adopted in Level-2 procedure of ASME B31G [10] and API 579 [13].

For a flat-bottomed corrosion, Eq. (16) becomes:

$$P_b = \frac{2t\sigma_f}{D} \left[\frac{1-(d/t)}{1-(d/t)/M} \right] \quad (17)$$

If a corrosion defect is long enough, $1/M$ approaches zero and Eq. (17) reduces to Eq. (12). In 1992, Richie and Last [38] adapted Eq. (17) as a corrosion acceptance criterion, that is, Shell-92 model, which used a flow stress $\sigma_f = 0.9\sigma_{uts}$. On this basis, Canadian standard SCA Z662 [34] was developed.

3.1.4. Comparison of the first-generation models

Figures 5(a) and 5(b) compares the first-generation models discussed above for a corrosion defect with depth of $d/t = 0.5$ and for two pipeline steels X52 and Gr. B, where the burst pressure P_b is normalized by the Barlow strength P_0 in Eq. (1). In these figures, five models are compared: *ASME B31G*, *Mod B31G*, *RSTRENG*, *Shell-92* and *CSA Z662*. The models utilized SMYS and the specified minimum tensile stress (SMTS).

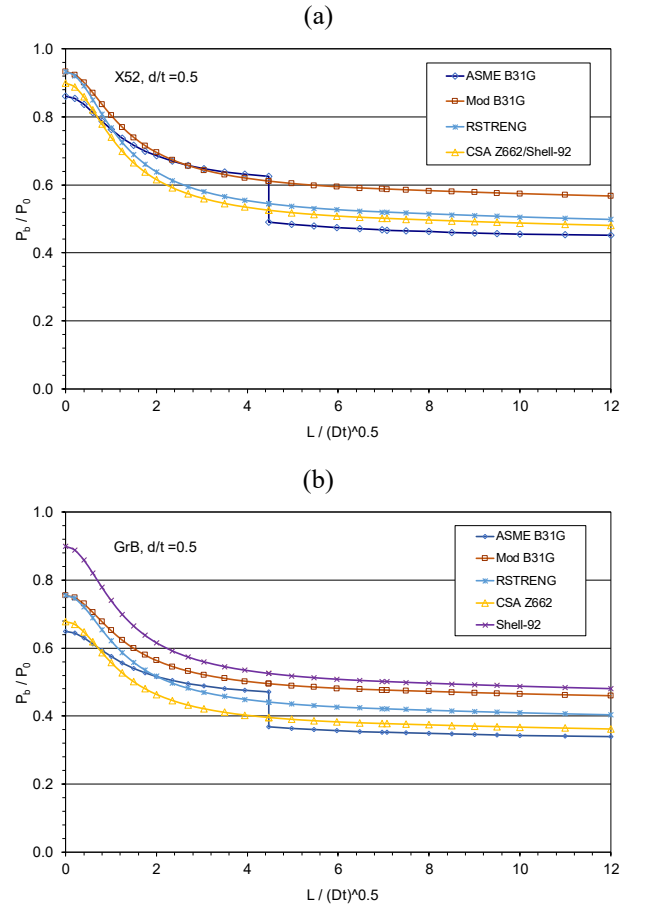


Figure 5. Comparison of the first-generation corrosion models for (a) X52, and (b) Gr. B

For X52, Fig. 5(a) shows that Mod B31G predicts the highest result for all defect lengths; CSA Z662 and Shell-92 are identical with predictions slightly lower than the RSTRENG results; and B31G predicts a comparable result to Mod B31G for a short corrosion defect, but the lowest result for a long corrosion defect. For Gr. B, Fig. 5(b) shows that the Shell-92 model

predicts the highest result over the entire defect length, and it is followed in order by Mod B31G, RSTRENG, and CSA Z662 models. ASME B31G model may predict comparable results to RSTRENG for short corrosion defects, but the lowest result for a long corrosion defect.

3.2. The second-generation models (1990s-2000s)

The second-generation corrosion models were developed numerically from finite element analysis (FEA) and simulation in the 1990s to 2000s with $S_R = UTS$.

3.2.1. LPC model

Based on a series of elastic-plastic FEA results and burst test data for X65 corroded pipes, a line pipe corrosion (LPC) model was developed at British Gas in 1995 [35-36] for determining burst pressure of corroded thin-walled pipes:

$$P_b = \frac{2t\sigma_{uts}}{D-t} \left[\frac{1-d/t}{1-d/Qt} \right] \quad (18)$$

where σ_{uts} is the UTS, and Q is a curve-fit bulging factor from the FEA results:

$$Q = \sqrt{1 + 0.31 \left(\frac{L}{\sqrt{Dt}} \right)^2} \quad (19)$$

The LPC criterion was adopted into DNV RP-F-101 [37] in 1999 with $S_R = 0.9UTS$ and statistical analysis, and then adopted in BS7910-1999 [12] with $S_R = (\sigma_{ys} + \sigma_{uts})/2$.

3.2.2. PCORRC model

In parallel to the LPC development, a pipeline corrosion criterion (PCORRC) was developed at Battelle in 1997 [38-39]:

$$P_b = \frac{2t\sigma_{uts}}{D} \left[1 - \frac{d}{t} \left(1 - \exp \left(-0.157 \frac{L}{\sqrt{D(t-d)/2}} \right) \right) \right] \quad (20)$$

For a very long corrosion defect, Equation (20) reduce to a simple equation:

$$p_b = \frac{2t\sigma_{uts}}{D} \left[1 - \frac{d}{t} \right] \quad (21)$$

If a defect is absent, Eq. (21) reduces to Eq. (1), that is, the Barlow strength for defect-free pipes.

Based on full-scale burst test data and FEA results for X70 corroded pipes, Yeom et al. [40] recalibrated the PCORRC model in 2015 with a factor 0.224 to replace 0.157 and a reference stress of $0.9UTS$ to replace UTS . In 2003, Choi et al. [41] developed another corrosion burst model based on their full-scale tests and FEA results for X65 corroded pipes.

3.2.3. Comparison of the second-generation models

Figure 6 compares the second-generation models discussed above for a flat defect with a depth of $d/t=0.5$ in X65 pipeline, where the material properties were assumed to be the SMYS and SMTS. In this figure, six models are compared: LPC (DNV), BS7910, PCORRC, Choie (2003), and Reformulated PCORRC by Yeom (2015). For comparison, RSTRENG and CSA Z662 are also included in Fig. 6. This figure shows that 1) LPC and PCORRC predict comparable results, 2) BS7910 and RSTRENG

predict similar results that are lower than those by LPC, 3) CSA Z662 and Yeom (2015) predict comparable results that are lower than RSTRENG predictions, and 4) Choi (2003) and Yeom (2015) are comparable for short defects and become nearly identical to be the lower bound for long defects.

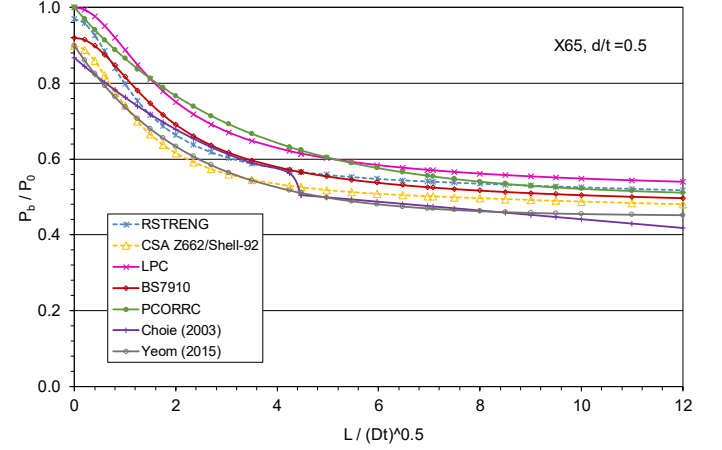


Figure 6. Comparison of the 2nd-G corrosion models for X65

3.3. The third-generation models (2000 to present)

The third-generation models considered the material strain hardening effect. These models are still being developed. The reference stress of these models is a function of UTS and n , that is, $S_R = f(UTS, n)$. Recently, Zhu [15] assessed seven third-generation models, and three of the most accurate are considered in this section.

3.3.1. Modified PCORRC model with Zhu-Leis flow solution

In 2018, Zhu [42] modified the PCORRC model with use of the Zhu-Leis flow solution in Eq. (6) for defect-free pipes to define the reference stress. The defect geometry function was assumed unchanged for corrosion defects with flat bottoms. The Mod-PCORRC model was expressed as:

$$p_b = \left(\frac{2+\sqrt{3}}{4\sqrt{3}} \right)^{n+1} \frac{4t\sigma_{uts}}{D} \times \left(1 - \frac{d}{t} \left(1 - \exp \left(-\frac{0.157L}{\sqrt{D(t-d)/2}} \right) \right) \right) \quad (22)$$

3.3.2. Modified LPC model with Zhu-Leis flow solution

In 2021, Zhu [15] further modified the LPC model with use of the Zhu-Leis flow solution in Eq. (6) for defect-free pipes to define the reference stress. The defect geometry function was also assumed unchanged for corrosion defects with flat bottoms. The Mod-PCORRC model was expressed as:

$$p_b = \left(\frac{2+\sqrt{3}}{4\sqrt{3}} \right)^{n+1} \frac{4t\sigma_{uts}}{D-t} \left[\frac{1-d/t}{1-d/Qt} \right] \quad (23)$$

3.3.3. A polynomial corrosion model

In 2015, Zhu [17] developed a new corrosion model that is different from any existing model. The reference stress was defined from the Zhu-Leis solution in Eq. (6) for defect-free pipes, and the defect geometry term determined from FEA

results contains a polynomial that is easier for engineers to apply. This polynomial corrosion model was expressed as:

$$P_b = \left(\frac{2+\sqrt{3}}{4\sqrt{3}}\right)^{n+1} \frac{4t\sigma_{uts}}{D} \left[1 - \frac{d}{t} \left(1 - \frac{1}{g\left(\frac{L}{\sqrt{Dt}}\right)}\right)\right] \quad (24)$$

where g is a polynomial function with a degree of 2:

$$g = 1 + 0.1385 \frac{L}{\sqrt{Dt}} + 0.1357 \left(\frac{L}{\sqrt{Dt}}\right)^2 \quad (25)$$

3.3.4. Validation of the third-generation models

Those third-generation corrosion models may be evaluated using a set of reliable full-scale test (FST) data for machined defects with flat bottoms in a Korean X65 pipeline steel [43]. The burst pressure data were reported for six defects with a fixed uniform depth of $d/t = 0.5$ and six lengths of $L = 50, 100, 200, 300, 600,$ and 900 mm. The pipe diameter is 762 mm (30 in.) and the wall thickness is 17.5 mm (0.69 in.). The actual YS and UTS of the X65 pipe are 495 MPa and 565 MPa. Figure 7 compares the burst pressure predictions from the three third-generation models with the test data for machined defects in the X65 pipe, where all burst pressures are normalized by the mean diameter-based Barlow strength P_0 .

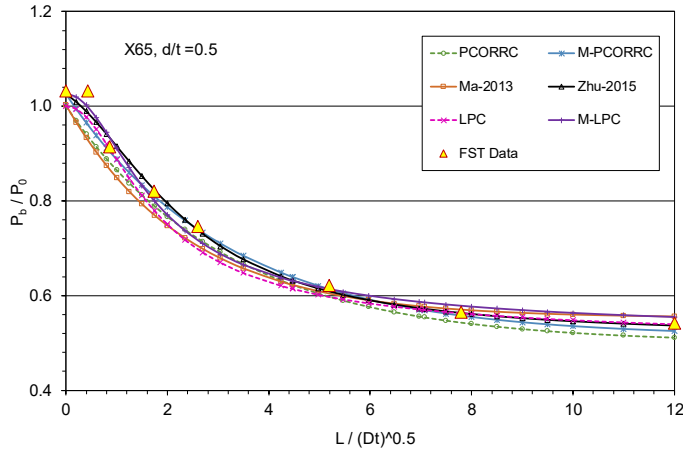


Figure 7. Comparison of 3rd-generation corrosion model predictions with burst test data

Also included in Fig. 7 are burst pressure predictions from the LPC, PCORRC, and another third-generation model proposed by Ma et al. [44] in 2013. This figure shows that all those models predict comparable results that closely match the burst test data for all defects in consideration. However, further observation indicates that (1) PCORRC is slightly conservative for all defects, (2) LPC is conservative for short defects, (3) Ma-2013 is conservative for short defects and slightly non-conservative for long defects, (4) Mod-LPC is accurate for short defects and slightly non-conservative for long defects, and (5) Zhu-2015 and Mod-PCORRC are nearly identical to each other and the most accurate in comparison to the FST data. Moreover, using a large number of full-scale burst test data, Ma et al. [44]

showed their model is accurate for mid to high strength steels, but less accurate for low-strength steels.

Recently, after experimental comparison and statistical analysis, Amaya-Gomez et al. [20] confirmed that Ma-2103 is inaccurate for low-strength steels, and Zhu-2015 polynomial model is more accurate to predict burst pressure for corroded pipelines, particularly for mid to high-strength steels. Using the PRCI full-scale burst test database for machined defects with flat bottoms, Leis [45] demonstrated that the Mod-PCORRC model in Eq. (22) is more accurate in predicting the remaining strength of corroded pipelines for a wide range of grades.

4. CORROSION MODELS FOR THICK-WALLED PIPES

4.1. Developing corrosion models for thick-walled pipes

A corrosion model for a thick-walled pipe is proposed by combining the reference stress for defect-free thick-walled pipes and the defect geometry function for corroded thin-walled pipes. It is similar to Eq. (10) in Section 3 that a general expression of burst pressure for a corrosion defect in a thick-walled pipeline can be expressed as follows:

$$P_b = S_R \times \ln\left(\frac{D_o}{D_i}\right) \times f(\text{defect geometry}) \quad (26)$$

In the above equation, the S_R is the burst strength for defect-free pipes in terms of the Zhu-Leis flow theory, that is:

$$S_R = 2 \left(\frac{2+\sqrt{3}}{4\sqrt{3}}\right)^{n+1} \sigma_{uts} \quad (27)$$

In fact, the S_R may be considered as a two-parameter (UTS and n) flow stress of the pipeline steel, which is independent of the pipe or defect geometry. In the absence of a defect, the defect geometry function, f , is 1, and Eq. (26) reduces to Eq. (8) as the Zhu-Leis flow solution for defect-free thick-walled pipes.

For a corrosion defect in a thick-walled pipe, it is assumed that the defect geometry function of a corrosion model for a thick-walled pipe is approximately the same as that for a thin-walled pipe. Thus, three corrosion models discussed in Section 3.3, including Mod-PCORRC model in Eq. (22), Mod-LPC model in Eq. (23), and the polynomial model in Eq. (24) are adapted as new corrosion models for thick-walled pipes:

$$p_b = 2 \left(\frac{2+\sqrt{3}}{4\sqrt{3}}\right)^{n+1} \sigma_{uts} \ln\left(\frac{D_o}{D_i}\right) \left(1 - \frac{d}{t} \left(1 - \exp\left(-\frac{0.157L}{\sqrt{D(t-d)/2}}\right)\right)\right) \quad (28)$$

$$p_b = 2 \left(\frac{2+\sqrt{3}}{4\sqrt{3}}\right)^{n+1} \sigma_{uts} \ln\left(\frac{D_o}{D_i}\right) \left[\frac{1-d/t}{1-d/Qt}\right] \quad (29)$$

$$P_b = 2 \left(\frac{2+\sqrt{3}}{4\sqrt{3}}\right)^{n+1} \sigma_{uts} \ln\left(\frac{D_o}{D_i}\right) \left(1 - \frac{t}{D}\right) \left[1 - \frac{d}{t} \left(1 - \frac{1}{g\left(\frac{L}{\sqrt{Dt}}\right)}\right)\right] \quad (30)$$

These corrosion models are applicable to thick-walled pipes and should have a higher degree of accuracy than the thin-wall corrosion models in Eqs (22), (23) and (24), as discussed next.

4.2. Experimental validation of thick-wall models

A large burst test database [45] containing 80 full-scale burst tests are employed here to evaluate and then validate the proposed corrosion models for thick-walled pipes. The full-scale burst tests involves machined defect features with flat bottoms in pipeline steels with grades of X46, X52, X60, X65, X70, X80, and X100. The tested pipe diameters ranged from 8.63 to 52 inches (219 to 1321 mm), with wall thicknesses that ranged from 0.233 to 1.0 inches (5.92 to 25.4 mm). Thus, the D/t ratios ranged from 8.6 to 81.8. Among these pipes, seven of them have small diameters and heavy walls, resulting in $D/t \approx 9$. Many of these burst tests considered a large range of defect depths and lengths, some metal loss defects were quite wide in comparison to their length.

For the convenience of comparison, the proposed corrosion models in Eqs (28), (29) and (3) are referred hereafter to as SRNL-PCORRC, SRNL-LPC and SRNL-Polynomial models. Since the burst test reports did not provide the values of strain hardening exponent n for the tested pipeline steels, all n values are estimated from an approximate equation using the yield to tensile strength (Y/T) ratio of the material [22]. Note that the estimated n values may cause certain errors in burst pressure predictions from Eqs (28) to (30).

4.2.1. Validating SRNL-PCORRC model

Figure 8(a) directly compares the burst pressure prediction from the PCORRC and SRNL-PCORRC models with the full-scale burst test data and Figure 8(b) compares the predicted to measured burst pressure ratio varied with the defect depth d/t ratio. Also included in these two figures are the burst pressure predictions from ASME B31G and Modified B31G. In Fig. 8(a), there are seven test data points with measured burst pressures larger than 10 ksi (68.95 MPa), and those test data were obtained for the small diameter, heavy-walled pipes with $D/t \approx 9$. From the comparisons in these two figures, the following observations are made:

- (1) B31G model generally predicts the most conservative burst pressure for almost all thick and thin-walled pipes, except for very deep defects with a d/t ratio close to 0.8. However, there are cases for which the B31G model overestimates burst pressure and leads to nonconservative predictions.
- (2) Modified B31G improves B31G predictions for most tests and reduces the conservatism. However, it can also predict nonconservative results for some tests.
- (3) The PCORRC model significantly improves both the B31G and the Modified B31G models and predicts more accurate burst pressures for thin-walled pipes on average. However, it considerably underestimates the burst pressures for thick-walled pipes.
- (4) The SRNL-PCORRC model further improves the PCORRC model and predicts more accurate burst pressures for both thin and thick-walled pipes with corrosion defects.
- (5) All models are inaccurate for deep defects at $d/t \approx 0.8$.

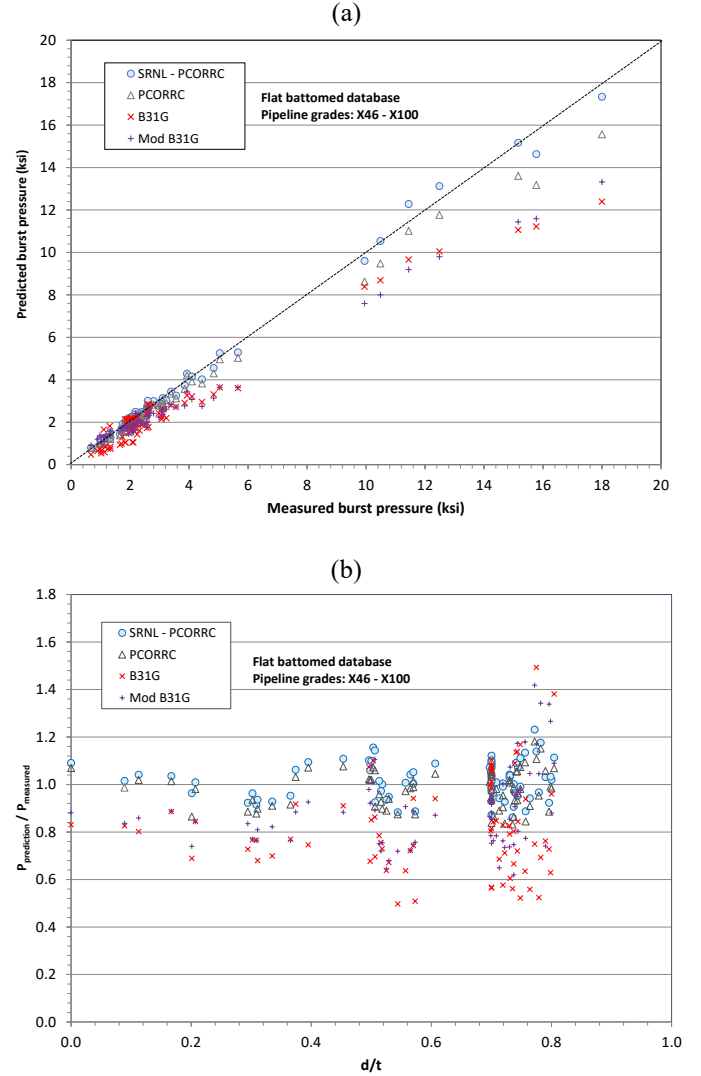


Figure 8. Comparison of PCORRC and SRNL-PCORRC model predictions with experimental burst data: (a) direct comparison, and (b) the pressure ratio as a function of d/t

4.2.2. Validating SRNL-LPC model

Figure 9(a) directly compares the burst pressure prediction from the LPC and SRNL-LPC models with the full-scale burst test data, while Figure 9(b) compares the predicted to measured burst pressure ratio varied with the defect depth d/t ratio. Also included in these two figures are the burst pressure predictions of ASME B31G and Modified B31G. From the comparisons in these two figures, the same observations made in Section 4.2.1 on the B31G and Modified B31G models are unchanged here, and the other observations are:

- (1) The LPC model significantly improves both B31G and Modified B31G models and can predict more accurate burst pressures for both thin and thick-walled pipes. However, it can overestimate burst pressures for deep defects at $d/t \approx 0.8$.

- (2) The SRNL-LPC model further improves LPC model and predicts improved results for thin and thick-walled pipes.
- (3) All models are inaccurate for deep defects at $d/t \approx 0.8$.

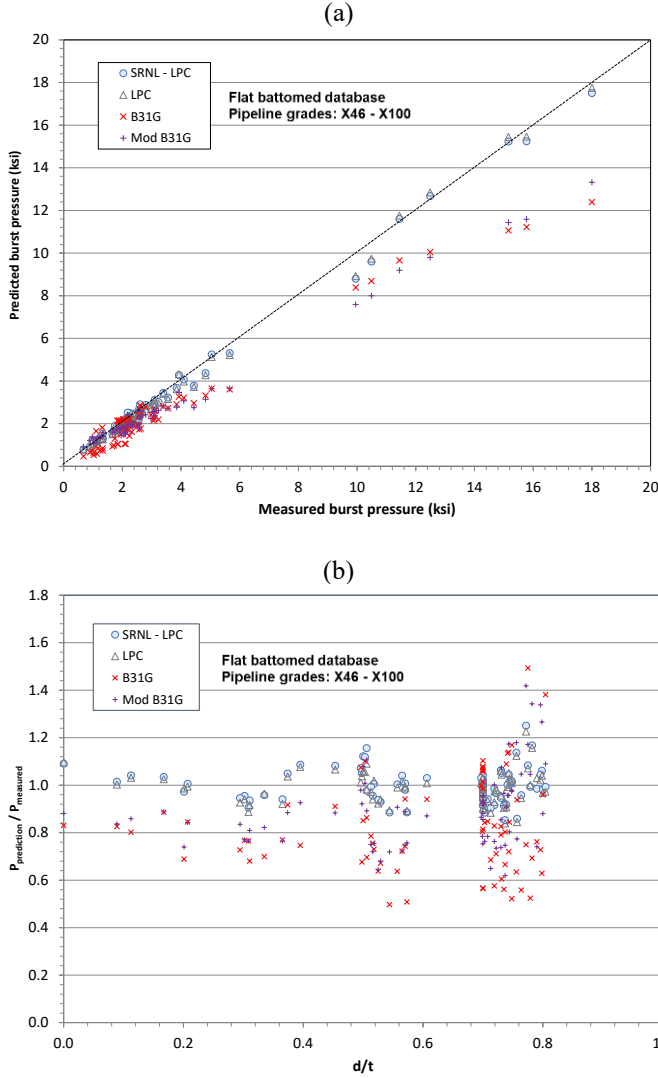


Figure 9. Comparison of LPC and SRNL-LPC model predictions with experimental burst data: (a) direct comparison, and (b) the pressure ratio as a function of d/t

4.2.3 Validating SRNL-Polynomial model

Figure 10(a) directly compares the burst pressure prediction from the PCORRC and SRNL-Polynomial models with the full-scale burst test data, while Figure 10(b) compares the predicted to measured burst pressure ratio varied with the defect depth d/t ratio. Also included in these two figures are the burst pressure predictions of ASME B31G and Modified B31G. From the comparisons in these two figures, the same observations made in Section 4.2.1 on the B31G, Modified B31G and PCORRC models are unchanged, and the other observations are:

- (1) The SRNL-Polynomial model improves PCORRC results for both thin and thick-walled pipes.
- (2) All models are inaccurate for deep defects at $d/t \approx 0.8$.

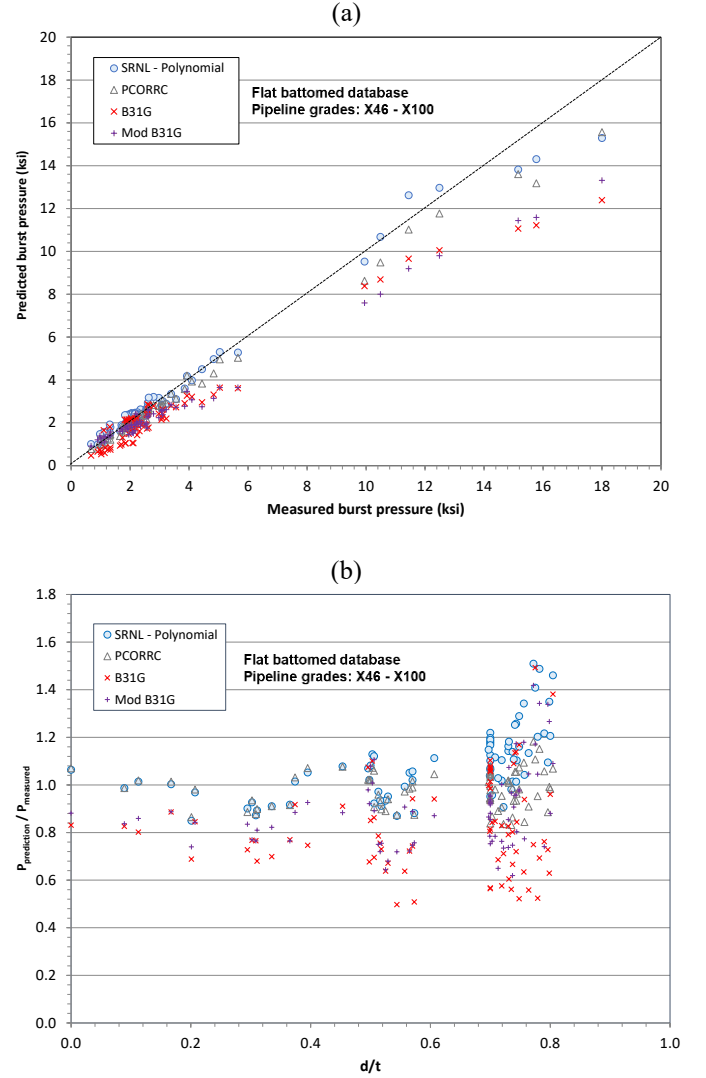


Figure 10. Comparison of PCORRC and SRNL-Polynomial model predictions with experimental burst data: (a) direct comparison, and (b) the pressure ratio as a function of d/t

4.2.4. Comparison of statistical model errors

In reference to the predicted to measured pressure ratio, statistical measures of variability for all prediction models were calculated, as listed in Table 1, including mean, standard error, and coefficient of variation (COV). It is clear from Table 1 that (1) B31G and Mod B31G have a large bias and a large uncertainty as quantified by COV, (2) LPC has a less bias and a small uncertainty than PCORRC, (3) SRNL-PCORRC has a slightly smaller bias and uncertainty than PCORRC, (4) SRNL-LPC has the least bias, and (5) SRNL-Polynomial has a reduced bias and uncertainty compared to B31G and Modified B31G.

Table 1. Statistical model errors

Model	Eq.	Mean	Std err	COV(%)
ASME B31G	(11)	0.822	0.200	24.3
Mod B31G	(14)	0.896	0.163	18.2
PCORRC	(20)	0.978	0.079	8.0
SRNL-PCORRC	(28)	1.020	0.079	7.8
LPC	(18)	0.988	0.063	6.9
SRNL-LPC	(29)	0.999	0.073	7.4
SRNL-Polynomial	(30)	1.084	0.146	13.4

Coupling the statistical results in Table 1 with the observations made in Sections 4.2.1 to 4.2.3, it is recommended that (1) LPC and PCORRC may be used to predict an accurate burst pressure for thin-walled pipes with corrosion defects of $d/t < 0.8$, (2) SRNL-LPC is slightly more accurate than SRNL-PCORRC, and both models predict comparable results for thick-walled pipes with corrosion defects of $d/t < 0.8$, and (3) SRNL-Polynomial can predict a more accurate burst pressure for thick-walled pipes with corrosion defects of $d/t < 0.7$.

5. CONCLUSIONS

This paper briefly reviewed the typical burst pressure models for defect-free thin-walled and thick-walled pipelines as well as examples of corrosion assessment models for corroded thin-walled pipelines. On this basis, three corrosion assessment models were developed for predicting remaining strength of corroded thick-walled pipelines in terms of the average shear stress yielding theory (i.e., Zhu-Leis theory). Subsequently, a large burst test database, with a wide range of pipeline steels, was utilized to evaluate the proposed corrosion assessment models for corroded thick-walled pipelines with a wide range of pipeline grades. Comparisons indicate that the proposed corrosion models for thick-walled pipes can predict more accurate remaining strength for corroded thin-walled and thick-walled pipelines. As a result, the proposed corrosion assessment models were validated by the full-scale test data.

From the statistical error analysis, it is recommended that:

- (1) Both LPC and PCORRC models can be used to predict accurate burst pressure for thin-walled pipes with corrosion defects of $d/t < 0.8$.
- (2) SRNL-LPC model is slightly more accurate than SRNL-PCORRC model, and both models predict comparable results for thick-walled pipes with corrosion defects of $d/t < 0.8$.
- (3) SRNL-Polynomial can predict more accurate burst pressure for thick-walled pipes with corrosion defects of $d/t < 0.7$.

ACKNOWLEDGEMENTS

The present author is grateful to the financial support by the Department of Energy (DOE) and its Laboratory Directed

Research and Development (LDRD) program through the LDRD Project 2022-00077 at Savannah River National Laboratory.

REFERENCES

- [1] Ossai CL, Boswell, B. Davies IJ, Pipeline Failure in Corrosive Environments – A Conceptual Analysis of Trends and Effects, *Engng Fail Anal*, 53; 2015: 36-58.
- [2] Christopher T, Sarma BS, Potti PK. A Comparative Study on Failure Pressure Estimation of Unflawed Cylindrical Vessels, *Int J Press Vessels Pip*, 79 (2002) 53-66.
- [3] Zhu XK, Leis BN. Evaluation of Burst Pressure Prediction Models for Line Pipes, *Int J Press Vessels Pip*, 89 (2012) 85-97.
- [4] Zhu XK, Leis BN. Accurate Prediction of Burst Pressure for Line Pipes, *J Pipeline Integrity*, 4; 2004: 195-206.
- [5] Zhu XK, Leis BN. Average Shear Stress Yield Criterion and Its Application to Plastic Collapse Analysis of Pipelines, *Int J Press Vessels Pip*, 83; 2006: 663-671.
- [6] Zhu XK. Strength Criteria versus Plastic Flow Criteria Used in Pressure Vessel Design and Analysis, *J Press Vessel Technol*, 138 (2016) 041402.
- [7] Keifner JF, Atterbury TJ, *Investigation of The Behavior of Corroded Line Pipe*, Project 216 Interim Report, February 1971.
- [8] Maxey WA, Kiefner JF, Eiber RJ, Duffy AR. Ductile Fracture Initiation, Propagation and Arrest in Cylindrical Vessels, *Fracture Toughness*, ASTM STP 514, Part II, 1972, pp. 347-362.
- [9] Kiefner JF, Maxey WA, Eiber RJ, Duffy AR. Failure stress levels of flaws in pressurized cylinders, *Progress in Flaw Growth and Fracture Toughness Testing*, ASTM STP 536, American Society for Testing and Materials, 1973: 461-481.
- [10] ASME B31G-2009, *Manual for Determining the Remaining Strength of Corroded Pipelines*, American Society of Mechanical Engineers, New York, USA, 2009.
- [11] Cosham A, Hopkins P, Macdonald KA. Best Practice For The Assessment of Defects in Pipelines, *Engng Fail Anal*, 14, (2007) 1245-1265.
- [12] BS 7910:2013 + A1:2015, *Incorporating Corrigenda Nos. 1 and 2 Guide on Methods for Assessing the Acceptability of Flaws in Metallic Structures*, British Standards Institution, London, UK, 2015.
- [13] API 579-1/ASME FFS-1, *Fitness for Service*, Third Edition, June 2016.
- [14] Zhu XK, Assessment methods and technical challenges of remaining strength for corrosion defects in pipelines, *Proceedings of the ASME Pressure Vessels and Piping Conference*, Prague, Czech, July 15-20, 2018.
- [15] Zhu XK. A Comparative Study of Burst Failure Models for Assessing Remaining Strength of Corroded Pipelines, *J Pipeline Science and Engineering*, 1, 2021: 36-50.
- [16] Zhu XK, Wiersma B. Progress of Assessment Model Development for Determining Remaining Strength of Corroded Pipelines, *Proceedings of the ASME 14th*

- International Pipeline Conference*, IPC2022-86922, September 26-30, 2022, Calgary, Alberta, Canada.
- [17] Zhu XK, A new material failure criterion for numerical simulation of burst pressure of corrosion defects in pipelines, *Proceedings of the ASME pressure vessels and Piping Conference*, Boston, Massachusetts, USA, July 19-23, 2015.
- [18] Leis BN, Zhu XK, Orth F, Aguiar D, Perry L. Minimize model uncertainty in current corrosion assessment criteria, *PRCI-APGA-EPRG 21th Joint Technical Meeting on Pipeline Research*, Colorado Springs, Colorado, USA, May 1-5, 2017
- [19] Zhou W, Huang GX. Model error assessments of burst capacity models for corroded pipelines, *Int J Press Vessels Pip*, 99-100; 2012: 1-8.
- [20] Amaya-Gomez R, et al. Reliability assessments of corroded pipelines based on internal pressure – A review, *Eng Fail Anal*, 98; 2019: 190-214.
- [21] Bhardwaj U, Teixeira AP, Soares CG. Uncertainty quantification of burst pressure models of corroded pipelines, *Int J Press Vessels Pip*, 188; 2020: 104208.
- [22] Zhu XK, Leis BN, Influence of yield-to-tensile strength ratio on failure assessment of corroded pipelines. *J Press Vessel Technol*, 127; 2005: 436-442.
- [23] Seghier MEAB, Keshtegar B, Elahmoune B. Reliability analysis of low, mid and high-grade strength corroded pipes based on plastic flow theory using adaptive nonlinear conjugate map, *Eng Fail Anal*, 90; 2018: 245-261.
- [24] Zimmermann S, Marewski U, Hohler S, Burst pressure of flawless pipes, *3R Inter*, Special Edition, 46; 2007: 28-33.
- [25] Zhou W, Huang T. Model error assessment of burst capacity models for defect-free pipes, *Proceedings of International Pipeline Conference*, 2012, Calgary, Canada, Sept 25-28.
- [26] Bony M, Alamilla JL, Vai R, Flores E. Failure pressure in corroded pipelines based on equivalent solutions for undamaged pipe, *J Press Vessel Technol*, 132; 2010: 051001.
- [27] Lyons CJ, Race JM, Chang E, Cosham A, Wetenhall B, Barnett J. Validation of the NG-18 Equations for thick-walled pipelines, *Eng Fail Anal*, 112; 2020: 104494.
- [28] Zhu XK, Wiersma B, Sindelar R, Johnson WR. New Strength Theory and Its Application to Determine Burst Pressure of Thick-Wall Pressure Vessels, *Proceedings of the ASME Pressure Vessels and Piping Conference*, July 17-22, 2022, Las Vegas, Nevada, USA. PVP2022-84902.
- [29] Folias ES. An axial crack in a pressured cylindrical shell, *Int J Fract Mech*, 1; 1965: 104-113.
- [30] Coulson K.W, Worthingham RG. Standard damage assessment approach is overly conservative, *Oil and Gas J*, April 9, 1990.
- [31] Kiefner JF, Vieth PH. *A Modified Criterion for Evaluating the Remaining Strength of Corroded Pipe*, Final report on Project PR 3-805 to the Pipeline Research Committee of the American Gas Association, 1989.
- [32] Kiefner JF, Vieth PH, Roytman I. Continuing validation of RSTRENG, Pipeline Research Supervisory Committee, A.G.A Catalogue No. L51689, December 1996.
- [33] Ritchie D, Last S. Shell 92 – Burst criteria of corroded pipelines – defect acceptance criteria, *EPRG-PRCI 10th Biannual Joint Technical Meeting on Pipeline Research*, Cambridge, UK, 1995.
- [34] CSA Z662-19, *Oil and Gas Pipeline Systems*, Canadian Standards Association, Mississauga, Canada, 2019.
- [35] Fu B and Kirkwood MG, Determination of failure pressure of corroded line pipes using nonlinear finite element method, *Proceedings of the 2nd International Pipeline Technology Conference*, Vol.II, 1995, pp. 1-9.
- [36] Fu B, Batte AD. New methods for assessing the remaining strength of corroded pipelines, *EPRG/PRCI 12th Biennial Joint Technical Meeting on Pipeline Research*, Groningen, The Netherlands, 1999, Paper 28.
- [37] Det Norske Veritas, *Recommended Practice DNV-RP-F101 – Corroded Pipelines*, 2015.
- [38] Leis BN, Stephens DR, An alternative approach to assess the integrity of corroded line pipes – Part I: current status and Part II: alternative criterion, *Proceedings of the Seventh International Offshore and Polar Engineering Conference*, Honolulu, Hawaii, USA, May 25-30, 1997.
- [39] Stephens DR, Leis BN. Development of an alternative criterion for residual strength of corrosion defects in moderate-to-high toughness pipe, *Proceedings of International Pipeline Conference*, Calgary, Alberta, Canada, Oct 1-5, 2000.
- [40] Yeom KJ, Lee YK, OH KH, Kim WS. Integrity assessment of a corroded API X70 pipe with a single defect by burst pressure analysis, *Eng Fail Anal*, 57; 2015: 553-561.
- [41] Choi JB, Goo BK, Kim JC, et al. Development of limit load solutions for corroded gas pipelines, *Int J Press Vessels Pip*, 80; 2003: 121-128.
- [42] Zhu XK. Burst failure models and their predictions of buried pipelines, *Proceedings of the Conference on Asset Integrity Management – Pipeline Integrity Management under Geohazard Conditions*, Houston, Texas, USA, March 25-28, 2019.
- [43] Kim WS, Kim YP, Kho YT, Choi JB. Full scale burst test and finite element analysis on corroded gas pipeline, *Proceedings of the fourth International Pipeline Conference*, Calgary, Alberta, Canada, Sept 30 – Oct 3, 2002.
- [44] Ma B, Shuai J, Liu D, Xu K. Assessment on failure pressure of high strength pipeline with corrosion defects, *Eng Fail Anal*, 32; 2013: 209-219.
- [45] Leis BN. Continuing Development of Metal-Loss Severity Criteria – Including Width Effects, *Proceedings of the ASME International Pipeline Conference*, Calgary, AB, Canada, Sept 28 - Oct 2, 2020.